

# Field oriented control driver development based on BTS7960 for physiotherapy robot implementation

Andi Nur Halisyah<sup>1</sup>, Dimas Adiputra<sup>1</sup>, Ardiansyah Al Farouq<sup>2</sup>

<sup>1</sup>Department of Electrical Engineering, Faculty of Electrical Technology and Smart Industry, Institut Teknologi Telkom Surabaya, Surabaya, Indonesia

<sup>2</sup>Department of Computer Engineering, Faculty of Electrical Technology and Smart Industry, Institut Teknologi Telkom Surabaya, Surabaya, Indonesia

## Article Info

### Article history:

Received Oct 10, 2023

Revised Nov 2, 2023

Accepted Nov 12, 2023

### Keywords:

BTS7960

Controller

Field oriented control

Physiotherapy robot

Stroke rehabilitation

## ABSTRACT

In conjunction with sustainable development goal 3 (SDG 3), it is important to develop a national electrical component for physiotherapy robot development. This study aimed to develop an open-loop field-oriented control (FOC) driver utilizing BTS7960. The driver utilized three BTS7960s that produce sinewave with variable angular frequency ( $\omega$ ). The research then compared the open-loop FOC driver with electronics speed controller (ESC) performance to drive a brushless DC (BLDC) motor with an initial rotation per minute (RPM) of 400, 500, and 600. The main observation was RPM reduction when the BLDC motor was subjected to loads of 20, 35, 50, 65, and 80 gr. The result showed that the open-loop FOC driver performed better, especially on an 80 gr load. For an initial RPM of 600, the RPM reduced to 100 when controlled with an open-loop FOC driver, but lesser when controlled using ESC. The open-loop FOC driver produces higher torque on the BLDC motor so it could rotate with less reduction compared to ESC, which is evident. The open-loop FOC driver can be easily developed using BTS7960 with a settling time of 4 seconds. However future studies should still consider close-loop FOC drivers to achieve higher torque performance and faster transient response for physiotherapy robot applications.

*This is an open access article under the [CC BY-SA](https://creativecommons.org/licenses/by-sa/4.0/) license.*



## Corresponding Author:

Dimas Adiputra

Department of Electrical Engineering, Faculty of Electrical Technology and Smart Industry, Institut Teknologi Telkom Surabaya

Ketintang St., 156, Surabaya, East Java-60231, Indonesia

Email: adimas@ittelkom-sby.ac.id

## 1. INTRODUCTION

Sustainable development goals (SDGs) are the resolution and commitment of the government across nations to build a world where no one is left behind. SDG 3 discusses ensuring good health and well-being promotion for all people of all ages. Improving the medical facilities, especially for treating the deadly disease, such as stroke is a must to achieve SDG 3 [1]. The stroke can cause motoric function disability for its survivor. The patient can recover motoric function by participating in stroke rehabilitation in the form of physiotherapy [2]. Involvement of digital technology innovation for stroke rehabilitation improvement is commonly found nowadays as can be seen from the previous research, such as robotic [3], [4] and virtual reality [5], [6] for intensive and interesting assisted physiotherapy.

One of the important motoric impairments to be recovered is the ankle because it plays a pivotal role in walking gait activity. Ankle physiotherapy using robots for post-stroke patients has shown promising

results in improving gait and functional mobility. Wearable ankle robots, also known as exoskeletons, are a potential intervention for gait rehabilitation post-stroke. Preliminary findings suggest that these devices have certain clinical benefits for the treatment of hemiplegic gait post-stroke [7]. The treatment using the robotic involves diagnostic and therapy customization to maintain performance during rehabilitation [8]. The therapy customization usually combines passive stretching with active and resisted movement [9]. It is also possible to conduct harder training menus such as stair training using ankle robotics for stroke rehabilitation [10]. In summary, robotic ankle physiotherapy for post-stroke patients has shown potential in improving gait, functional mobility, and walking safety. However, further research and clinical trials are still needed to enhance the clinical effectiveness of wearable ankle robots and determine the best control strategies for robot-assisted post-stroke lower limb rehabilitation [7], [11].

Electrical components play a crucial role in the functioning of ankle physiotherapy robots. These robots typically use electric motors, pneumatic actuators, or electro-hydraulic systems as actuators to provide the necessary movement and force for ankle exercises [12]. Among them, electric motors are commonly used in both wearable and platform-based ankle physiotherapy robots due to their compact size, high efficiency, and precise control capabilities [13]. Other electrical components also include control systems, sensors, and power supplies [14], [15]. They work together to provide accurate, consistent, and engaging physiotherapy for patients recovering from ankle injuries [8].

The control systems are responsible for managing the robot's movements and ensuring that the therapy is accurate and consistent [16], [17]. Sensors are used to monitor the patient's ankle movements, joint angles, and forces exerted during therapy. This information is crucial for the control system to adjust the robot's movements and provide appropriate assistance or resistance during the exercises [18], [19]. Common sensors used in ankle rehabilitation robots include encoders, force sensors, and accelerometers [12], [20]. Power supplies provide the necessary electrical energy to operate the robot's actuators, control systems, and sensors. In wearable ankle rehabilitation robots, power supplies are often designed to be compact and lightweight to ensure the robot's portability and comfort for the patient [21].

The control system of an ankle physiotherapy robot must be capable, at least, of driving the actuator. Various control strategies have been reported in previous research for driving the electrical motor, especially the brushless DC (BLDC) motor, such as trapezoidal commutation and field-oriented control (FOC) that utilizes sinusoidal commutation. Trapezoidal commutation is one of the simplest methods for controlling BLDC motors. It uses square-wave currents to align with the motor's trapezoidal back electromotive force (back-EMF) profile for optimal torque generation. The current alignment is based on the Hall effect sensor reading. In some works, the Hall effect sensors can be discarded by employing sensorless control techniques by using the back-EMF of the motor to estimate the rotor position [22]. Also known as vector control, FOC is a mathematically advanced method for controlling the BLDC motor. It provides better efficiency and performance by decoupling the control of flux and torque [23]. The signal form is usually sinusoidal, thus the FOC is often associated with sinusoidal control. Implementation of sinusoidal control results in smoother motion and higher performance compared to trapezoidal commutation, which is suitable for medical applications [24].

FOC driver discussion is hardly found compared to the discussion on the algorithm. However, the driver can be developed by following these steps: choose a microcontroller, choose a motor driver, implement the FOC algorithm, and then design the PCB to start prototyping and testing. The microcontroller must be able to handle FOC algorithm computational requirements. Notable microcontrollers include Arduino, STM32, and ESP32. The motor driver must be able to handle the current and voltage requirements of the motor being used. There are several motor driver boards available that are designed for gimbal motors and work with the FOC algorithm, such as the SimpleFOCShield and the SimpleFOCPowerShield. Then, the developer must ensure that the driver can sense the current and position of the rotor because that information is compulsory to run closed-loop FOC.

The SimpleFOCShield board uses BTN8982 for driving the current. This component is rarely found in the Indonesian market, thus making the prototyping of FOC drivers challenging. Therefore, this study aims to build an FOC driver using an alternative component, which is BTS7960. Both BTN8982 and BTS7960 components have similar specifications. Because of that, an FOC driver is expected to be built using the BTS7960. For comparison purposes, the FOC driver using BTS7960 with an open-loop FOC algorithm is compared to the electrical speed control (ESC), which is commonly found in Indonesia. The research expects that the open-loop FOC driver using BTS7960 can perform better than the ESC to drive motor in terms of higher torque generated under the same rotation per minute (RPM).

## 2. METHOD

The FOC method for controlling a BLDC motor RPM is presented in Figure 1(a). The system achieves optimal torque whenever the phasor current ( $I_q$ ,  $I_d$ ) differs by 90 degrees phase. Firstly, the three-phase current of the BLDC motor ( $I_a$ ,  $I_b$ , and  $I_c$ ) is measured along with the angular position and RPM.

The RPM is compared with the RPM reference before being controlled using a proportional-integral (PI) controller. A current sensor is necessary for measuring the three-phase current, which then is transformed into the actual phasor current using Clarke and Park transform. The actual phasor current is compared to the phasor current reference (calculated based on the controlled RPM). Another PI controlled produces the controlled phasor current based on the error. Finally, after the controlled phasor current is transformed back into the three-phase current duty cycle, the BLDC motor is expected to move with the desired RPM.

Control of motor movement will impact the physiotherapy robot movement directly. Therefore, feedback control is essential to ensure robust intervention for the post-stroke patient [17]. However, this study only focuses on the open-loop process, as shown in Figure 1(b). No sensors and feedback are involved in this study. Hence, the proposed driver is called an open-loop FOC driver. The open-loop FOC driver receives angular frequency,  $\omega$  of a sine wave as the input. Then, the controller converts it into a duty cycle of the three-phase current to drive the BLDC motor accordingly. The RPM has a proportional relationship with the angular frequency. If the angular frequency is increased, then the RPM will also increase, and vice versa.

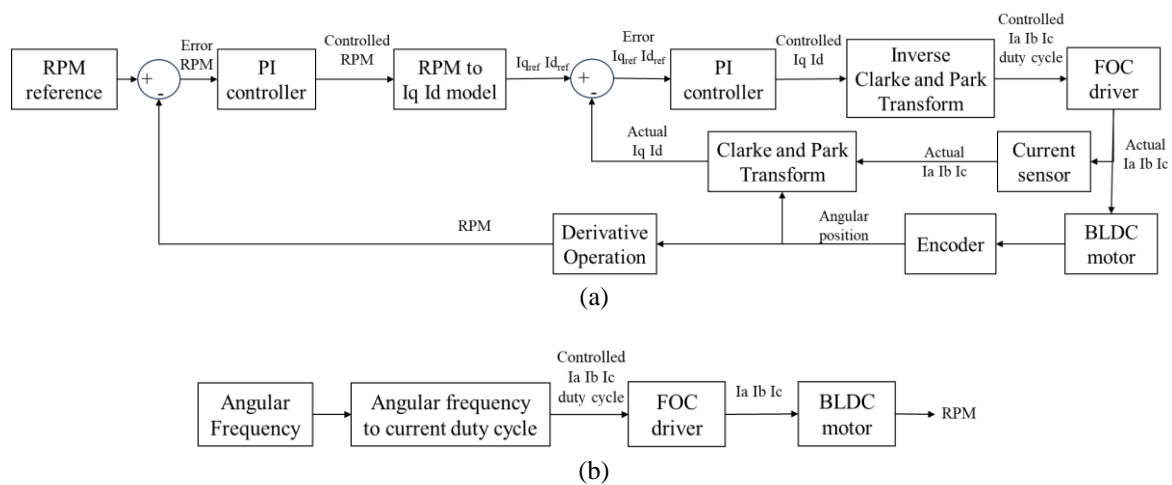


Figure 1. Block diagram of field oriented control method (a) close-loop system and (b) open-loop system

Two BLDC drivers are involved in this study, which is the ESC and open-loop FOC driver using BTS7960. The ESC is Xxd HW30A with a maximum operating voltage of 5 V and a maximum current of 30 A. Like the usual ESC, the power port consists of an input power port (positive and negative) and three phases of output, as shown in Figure 2(a). The output is connected accordingly to channels A, B, and C of the BLDC motor. For changing the direction, channels A and C can be swapped, while retaining the channel B connection. There is also a control port, where one pin is for getting a pulse width modulation (PWM) signal from the Arduino microcontroller (D9), and the other is connected to 5 V and the ground of Arduino. The PWM signal determines the frequency of the square wave output.

The BTS7960 is obtained from the IBT-2 H-Bridge module, which has a maximum operating voltage of 27 V and a maximum current of 43 A. It has a control port and a power port. The control port mainly consists of a power pin, an enable pin, and a PWM pin. The power pins connect to 5 V and the ground of the microcontroller. The enable pins should always be high. Then, the PWM pins connect to Arduino's PWM output. The power port consists of input pins and output pins. The output pins are M+ and M-, which are usually used to drive a DC motor. However, the voltage on these output pins can be controlled independently according to the PWM signal. For instance, the M+ voltage can be set to 5 V, while the M- can be set to 3 V. This ability opens the possibility to drive the three-phase signal to drive the BLDC motor.

Figure 2(b) shows the circuitry of the open-loop FOC drive utilizing the BTS7960 driver. There are three IBT-2 modules used, where each M+ pin represents one channel output to drive the BLDC motor. Likewise, the R\_EN pin is connected to 5V to enable only the M+ PWM pin or rather the RPWM pin. Each RPWM pin is connected to one PWM output of the microcontroller Arduino. In this case, pin digital 9, 10, and 11 have similar PWM signal frequencies of 490 Hz. Lastly, the 5V supply is connected to the input pins of all the IBT-2 modules (B+ and B-).

The ESC generates a current of a three-phase square wave signal. The signal amplitude is the same as the input voltage while the frequency is controllable according to the PWM duty cycles. Maximum duty

cycle means maximum frequency to drive the maximum angular speed of the BLDC motor. Meanwhile, the open-loop FOC driver generates a voltage of a three-phase sinusoidal signal.

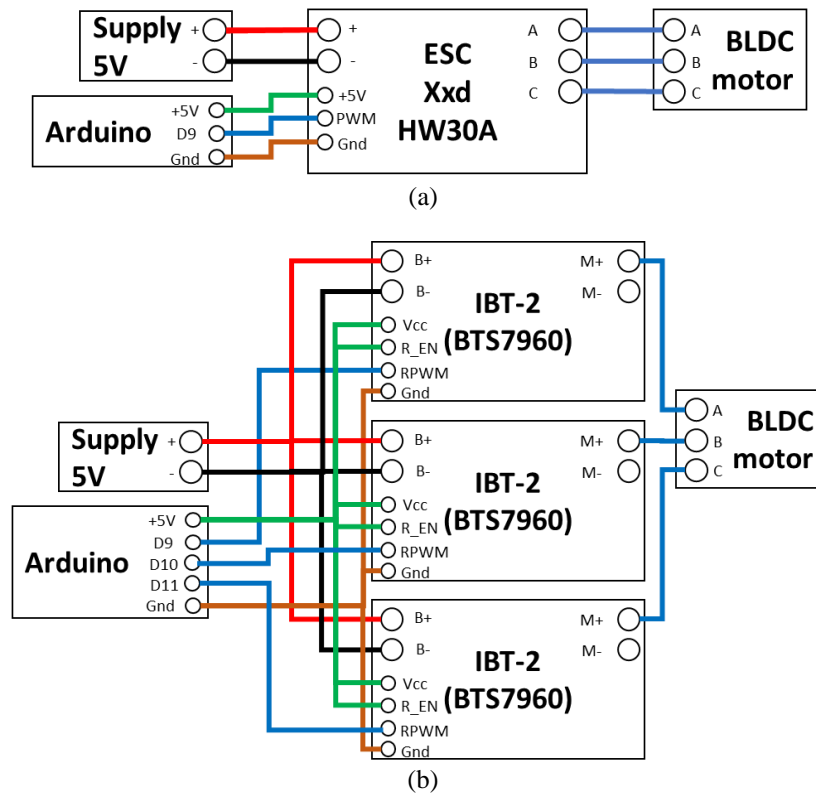


Figure 2. Circuitry of the (a) ESC and (b) open-loop FOC driver using BTS7960

$$V_A = \frac{V_{Peak}}{2} + \frac{V_{Peak}}{2} \sin(\omega t) \tag{1}$$

$$V_B = \frac{V_{Peak}}{2} + \frac{V_{Peak}}{2} \sin(\omega t + \frac{2}{3}\pi) \tag{2}$$

$$V_C = \frac{V_{Peak}}{2} + \frac{V_{Peak}}{2} \sin(\omega t + \frac{4}{3}\pi) \tag{3}$$

where  $V_A$ ,  $V_B$ , and  $V_C$  are the voltage on each motor BLDC channel, as shown in Figure 3(a), to drive the current.  $V_{Peak}$  is the input voltage, while  $\omega$  is the angular frequency of the sinusoidal signal. The  $V_{Peak}$  is generated by having maximum PWM duty cycles on the RPWM pin. Each channel's voltage should have a phase difference of 120 degrees ( $2/3\pi$  radians) so the developed driver can produce the necessary current to drive the BLDC motor as shown in Figure 3(b) [25], [26]. A star configuration as shown in Figure 2(c) is the assumption for the BLDC motor circuit, where the circuit is branched out into three lines. The assumption is the coil on each line got similar resistance like 1 Ohm all. Then the voltage on each line, as in  $V_A$ ,  $V_B$ , and  $V_C$  should have a different phase of 120 degrees. Following the Kirchoff Law, the current  $I_A$ ,  $I_B$ , and  $I_C$  can be calculated over time as shown in Figure 3(c). The order goes from  $V_A$ - $V_C$ - $V_B$  to become  $I_A$ - $I_B$ - $I_C$ . The maximum supply of 5 V produces a maximum current of 2.5 A in both directions. Minus current means the current goes back to the supply while positive current means the current goes from the supply.

The BLDC motor is a 5010 360 KV motor with an operating voltage from 5 to 24 V. The motor has dimensions of 50 mm in diameter and 10 mm in thickness. The motor dimension is small, thus suitable to be used in the context of an ankle physiotherapy robot. For the testing purpose of observing the motor's torque, an arm is attached to the BLDC motor that is rotating with load on its edge as shown in Figure 4. The load is varied, such as 20, 35, 50, 65, and 80 gr. The motor rotates at various angular speeds with and without the load. Then, the research measures the RPM difference before and after the load is applied. The RPM will reduce due to the load attached. The greater reduction in RPM means the less torque of the BLDC motor.

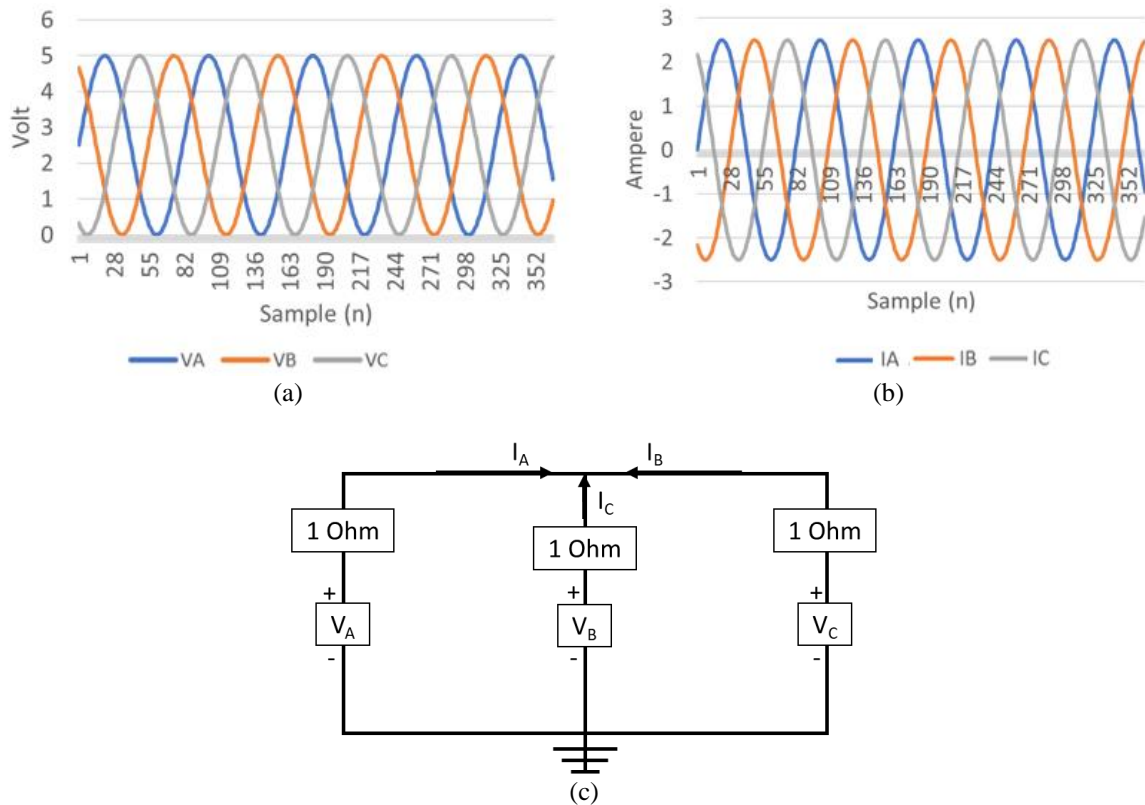


Figure 3. Open-loop FOC driver signal generation assumption (a) voltage on each channel, (b) generated current, and (c) star configuration of the BLDC motor

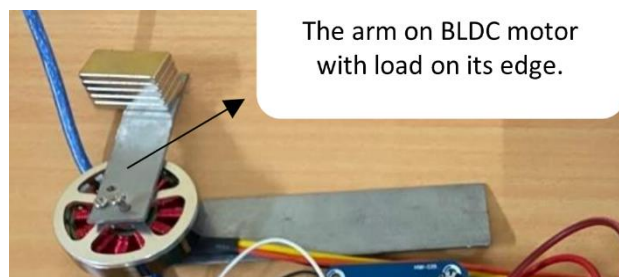


Figure 4. Experiment set up of the BLDC motor

The angular speed variations are 600 rpm, 500 rpm, and 400 rpm, which are measured using a tachometer. For the ESC, the PWM duty cycle is adjusted so the initial RPM can be achieved. As for the open-loop FOC driver, the  $\omega$  is adjusted so the motor can rotate with the initial RPM since the voltage is a function of the angular frequency. The transient response of the RPM is observed. Also, during the experiment, the power taken from the supply is monitored.

### 3. RESULTS AND DISCUSSION

Firstly, the transient response of the BLDC motor RPM is shown in Figure 5. When subjected to RPM reference input, both the open-loop driver and ESC can produce the desired RPM in 4 seconds, or the settling time ( $t_s$ ) is 4 seconds. This transient response is similar for all RPM references of 400, 500, and 600 RPM. Then, when subjected to load, the RPM reduction of the BLDC motor is apparent, as shown in Figures 6(a) to 8(b). The more weight the more the reduction on the BLDC motor RPM. However, different controls might result in different RPM reductions due to the motor torque achievement of each controller/driver being different.

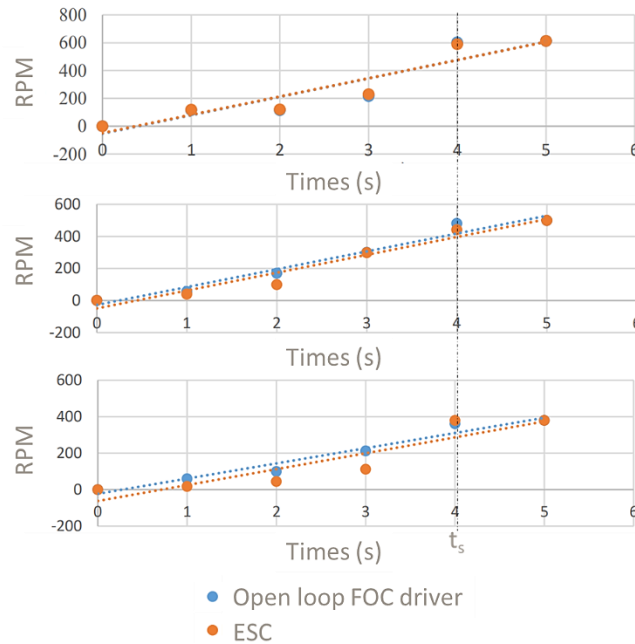


Figure 5. The transient response of the open-loop FOC driver and ESC

From an initial RPM of 600 as shown in Figure 6(a), the BLDC motor controlled with ESC reduces to about 580 RPM with a 20 gr load. Then, the RPM goes down to below 100 when the motor BLDC is subjected to an 80gr load. As for the BLDC motor with an open-loop FOC driver, the RPM reduces to about 540 RPM when the load is 20 gr and the RPM reduces to 100 RPM when the load is 80 gr. For the initial RPM of 500 as shown in Figure 7(a), the ESC-controlled RPM is 450 when the load is 20 gr and about 50 RPM when the load is 80 gr. The RPM is below 400 RPM and about 80 RPM when the BLDC motor is controlled using an open-loop FOC driver with a load of 20 and 80gr respectively. Also, for the initial RPM condition of 400 as shown in Figure 8(a), the ESC controlled produces RPM reduction to around 330 when the load is 20 gr and 50 when the load is 80 gr. On the other hand, the open-loop FOC driver-controlled BLDC motor RPM is about 310 and about 60 when the load is 20 gr and 80 gr respectively. This result suggests that the open-loop FOC driver has lower torque when the load is lighter but has higher torque when the load is heavier compared to the BLDC motor controlled with the ESC.

Meanwhile, in terms of power usage, the open-loop FOC driver uses more power compared to the ESC for driving the motor BLDC with various loads. For instance, the power usage of ESC is around 1.1 watts versus the open-loop FOC driver power usage is 1.5 watts as shown in Figure 6(b), initial RPM of 600, load of 80 gr). The trend is the same for all initial RPM conditions. However, there is a difference in maximum power usage. The lesser the initial RPM, the higher the power usage. In this case, when the initial RPM is 400, the power usage is about 2.7 watts when the load is 80gr as shown in Figure 8(b). Compared to other initial RPM conditions, which are 600 and 500, the power usage is around 1.5 watts and 2.4 watts respectively with the same load of 80gr as shown in Figures 6(b) and 7(b). The research also observes similar results with a different load, where the open-loop FOC driver uses more power compared to the ESC.

The initial RPM determines the torque of the BLDC motor [27]. Higher RPM means higher torque, as demonstrated in the result, where higher initial RPM resulted in lower RPM reduction, and this is true for both ESC and open-loop FOC driver controlled. For instance, when given a 20gr load, the RPM is still near 600 RPM when the initial RPM is 600 (less than 50 RPM reduction), but 400 to 450 RPM when the initial RPM is 500 (greater than 50 RPM reduction). For the higher load, the result also shows a similar observation. When the initial RPM is 600 with a load of 80gr, the RPM goes down to 100, but goes down to around 50 RPM when the initial RPM is 400.

Although the BLDC motor rotates with the same initial RPM, the RPM reduction is comparable when controlled with a different controller. The sinusoidal signal should excel in achieving higher torque compared to the square wave signal [28]. However, the result shows that the ESC seems superior for a lower load, but the open-loop FOC driver is superior for a higher load. One explanation is the nature of the sinusoidal signal it can generate full torque at zero speed [29]. This means that when the RPM is lower, the sinusoidal signal will exhibit higher torque achievement. On the other hand, when the RPM is higher, the

ESC performs better because the square wave signal is more suitable for high-speed operations, such as in drone applications (the usual RPM in each thruster is greater than 10,000 RPM) [30].

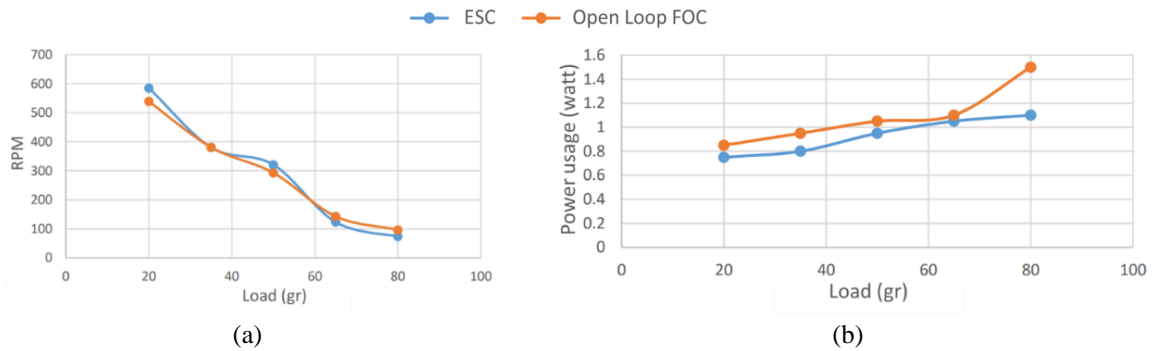


Figure 6. Comparison when the initial RPM is 600 (a) RPM and (b) power usage

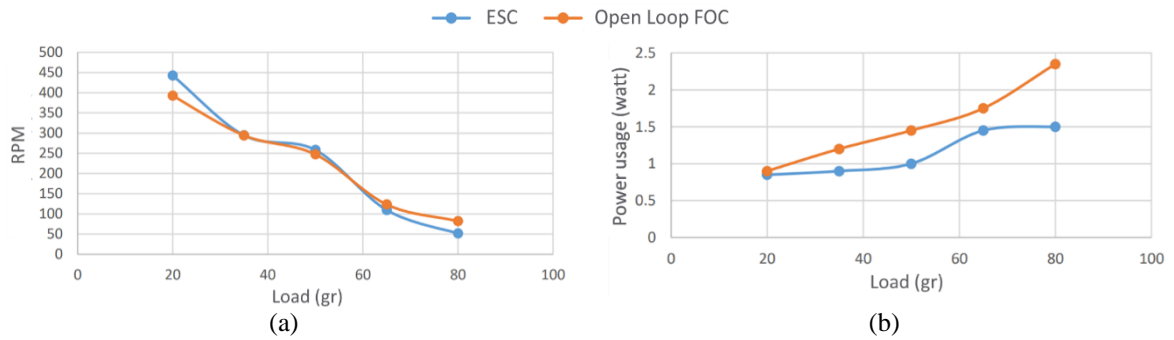


Figure 7. Comparison when the initial RPM is 500 (a) RPM and (b) power usage

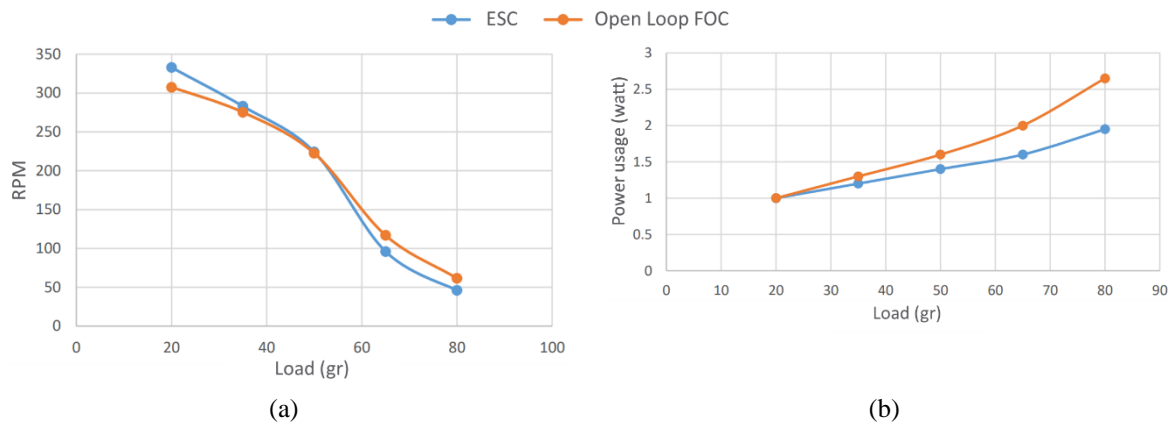


Figure 8. Comparison when the initial RPM is 400 (a) RPM and (b) power usage

The lower speed occurred when the load was heavier, and the higher speed occurred when the load was lighter. The open-loop FOC driver performs well for lower speeds with heavier loads, which is suitable for applications in physiotherapy robots. In most cases, physiotherapy involves slow rotational movement with high inertia because of the patient's spasticity [31], [32]. Typically, a robot for physiotherapy purposes is designed to rotate with RPM not more than 50 [33]. Because of that, the open-loop FOC driver shown in this study can be further utilized in developing a physiotherapy robot, such as the previous ankle robot by the authors [14].

However, it is important to note that the required torque for ankle application is at least 1 Nm [18]. The assumption is the robot should be able to lift the foot, which is 1.45% of the body weight [34]. For example, the typical body weight of Indonesians is 50 to 70 Kg. Then, the foot mass will be around 1 kg. Clearly, this study shows that the load is only 80 gr which is very far from 1 kg. Therefore, future studies can be focused on developing the close-loop FOC driver to achieve higher torque compared to the open-loop FOC driver presented in this study. Also, the control of the whole robotic system should be discussed since the robot is directly interacting with the amputee. For instance, the control algorithm for the user's gait. Proportional integral derivative (PID) control is not capable of controlling the gait due to the non-linearity aspect. A higher control algorithm is necessary for that task, such as a bio-inspired algorithm [35], or a supervised and reinforced algorithm [36]. In this case, the higher control algorithm can determine the control reference of the motor driver controller.

#### 4. CONCLUSION

An open-loop FOC driver is successfully developed in this study by utilizing three BTS7960 and Arduino microcontroller, which is commonly found in the Indonesian marketplace. Performance comparison between ESC and the developed open-loop FOC driver was done to justify the usage with other commonly found BLDC motor drivers in Indonesia. The result shows that the open-loop FOC driver is superior compared to ESC to drive the BLDC motor with a load of 80gr. When the initial RPM is 600, the BLDC motor RPM reduces to 100 RPM when controlled using an open-loop FOC driver but reduces to below 100 RPM when controlled using the ESC. The possible implementation of the open-loop FOC driver in physiotherapy robots is evidenced due to the higher torque in lower-speed applications. Future studies should consider the close-loop FOC driver development for better torque achievement. After that, if the motor actuation control is done, then the next step is to employ higher control algorithms for the gait control of the physiotherapy robot.

#### ACKNOWLEDGEMENTS

The authors would like to thank Institut Teknologi Telkom Surabaya for the financial support throughout the research under an internal research grant with contract number: 754/PNLT1/LPPM/VIII/2023.

#### REFERENCES




- [1] J. K. Goeller and K. Bartels, "Improving prediction to prevent perioperative morbidity," *British Journal of Anaesthesia*, vol. 127, no. 5, pp. 671–674, Nov. 2021, doi: 10.1016/j.bja.2021.08.004.
- [2] S. L. Whittaker, N. F. Taylor, K. D. Hill, C. L. Ekegren, and N. K. Brusco, "Self-managed occupational therapy and physiotherapy for adults receiving inpatient rehabilitation ('my therapy'): protocol for a mixed-methods process evaluation," *BMC Health Services Research*, vol. 21, no. 1, Aug. 2021, doi: 10.1186/s12913-021-06463-8.
- [3] Y.-H. Kim, "Robotic assisted rehabilitation therapy for enhancing gait and motor function after stroke," *Precision and Future Medicine*, vol. 3, no. 3, pp. 103–115, Sep. 2019, doi: 10.23838/pfm.2019.00065.
- [4] Y. Chen, K. T. Abel, J. T. Janeczek, Y. Chen, K. Zheng, and S. C. Cramer, "Home-based technologies for stroke rehabilitation: a systematic review," *International Journal of Medical Informatics*, vol. 123, pp. 11–22, Mar. 2019, doi: 10.1016/j.ijmedinf.2018.12.001.
- [5] W. E. Clark, M. Sivan, and R. J. O'Connor, "Evaluating the use of robotic and virtual reality rehabilitation technologies to improve function in stroke survivors: a narrative review," *Journal of Rehabilitation and Assistive Technologies Engineering*, vol. 6, Jan. 2019, doi: 10.1177/2055668319863557.
- [6] A. Demeco *et al.*, "Immersive virtual reality in post-stroke rehabilitation: a systematic review," *Sensors*, vol. 23, no. 3, Feb. 2023, doi: 10.3390/s23031712.
- [7] B. Shi *et al.*, "Wearable ankle robots in post-stroke rehabilitation of gait: a systematic review," *Frontiers in Neurobotics*, vol. 13, Aug. 2019, doi: 10.3389/fnbot.2019.00063.
- [8] M. N. Shah, S. N. Basah, K. S. Basaruddin, H. Takemura, E. J. Yeap, and C. C. Lim, "Ankle injury rehabilitation robot (AIRR): review of strengths and opportunities based on a SWOT (strengths, weaknesses, opportunities, threats) analysis," *Machines*, vol. 10, no. 11, Nov. 2022, doi: 10.3390/machines10111031.
- [9] G. Asín-Prieto *et al.*, "Post-stroke rehabilitation of the ankle joint with a low cost monoarticular ankle robotic exoskeleton: preliminary results," *Frontiers in Bioengineering and Biotechnology*, vol. 10, Nov. 2022, doi: 10.3389/fbioe.2022.1015201.
- [10] L. F. Yeung, C. C. Y. Lau, C. W. K. Lai, Y. O. Y. Soo, M. L. Chan, and R. K. Y. Tong, "Effects of wearable ankle robotics for stair and over-ground training on sub-acute stroke: a randomized controlled trial," *Journal of NeuroEngineering and Rehabilitation*, vol. 18, no. 1, Jun. 2021, doi: 10.1186/s12984-021-00814-6.
- [11] S. Campagnini, P. Liuzzi, A. Mannini, R. Riener, and M. C. Carrozza, "Effects of control strategies on gait in robot-assisted post-stroke lower limb rehabilitation: a systematic review," *Journal of NeuroEngineering and Rehabilitation*, vol. 19, no. 1, Jun. 2022, doi: 10.1186/s12984-022-01031-5.
- [12] I. Doroftei, C.-M. Cazacu, and S. Alaci, "Design and experimental testing of an ankle rehabilitation robot," *Actuators*, vol. 12, no. 6, Jun. 2023, doi: 10.3390/act12060238.
- [13] H. R. Jayetileke, W. R. De Mel, and H. U. W. Ratnayake, "A dynamic AI controller for a field-oriented controlled BLDC motor to achieve the desired angular velocity and torque," *International Journal of Intelligent Systems and Applications in Engineering*, vol. 7, no. 3, pp. 166–182, 2019, doi: 10.18201/ijisae.2019355379.
- [14] D. Adiputra *et al.*, "Robot ankle foot orthosis with auto flexion mode for foot drop training on post-stroke patient in Indonesia,"






- Kinetik: Game Technology, Information System, Computer Network, Computing, Electronics, and Control*, Nov. 2022, doi: 10.22219/kinetik.v7i4.1533.
- [15] D. Adiputra, U. Asfari, Ubaidillah, M. A. Abdul Rahman, and A. M. Harun, "Immediate effect evaluation of a robotic ankle-foot orthosis with customized algorithm for a foot drop patient: a quantitative and qualitative case report," *International Journal of Environmental Research and Public Health*, vol. 20, no. 4, p. 3745, Feb. 2023, doi: 10.3390/ijerph20043745.
- [16] M. Zhang, T. C. Davies, and S. Xie, "Effectiveness of robot-assisted therapy on ankle rehabilitation - a systematic review," *Journal of NeuroEngineering and Rehabilitation*, vol. 10, no. 1, 2013, doi: 10.1186/1743-0003-10-30.
- [17] M. W. Spong, "An historical perspective on the control of robotic manipulators," *Annual Review of Control, Robotics, and Autonomous Systems*, vol. 5, no. 1, pp. 1–31, May 2022, doi: 10.1146/annurev-control-042920-094829.
- [18] D. Adiputra, M. A. A. Rahman, Ubaidillah, and S. A. Mazlan, "Improving passive ankle foot orthosis system using estimated ankle velocity reference," *IEEE Access*, vol. 8, pp. 194780–194794, 2020, doi: 10.1109/ACCESS.2020.3033852.
- [19] D. Adiputra, M. Azizi Abdul Rahman, I. Bahiuddin, Ubaidillah, F. Imaduddin, and N. Nazmi, "Sensor number optimization using neural network for ankle foot orthosis equipped with magnetorheological brake," *Open Engineering*, vol. 11, no. 1, pp. 91–101, Nov. 2020, doi: 10.1515/eng-2021-0010.
- [20] Q. Meng, G. Liu, X. Xu, Q. Meng, and H. Yu, "Design and analysis of a supine ankle rehabilitation robot for early stroke recovery," *Machines*, vol. 11, no. 8, Jul. 2023, doi: 10.3390/machines11080787.
- [21] P. K. Jamwal, S. Hussain, N. Mir-Nasiri, M. H. Ghayesh, and S. Q. Xie, "Tele-rehabilitation using in-house wearable ankle rehabilitation robot," *Assistive Technology*, vol. 30, no. 1, pp. 24–33, Sep. 2018, doi: 10.1080/10400435.2016.1230153.
- [22] X. Yao, J. Zhao, G. Lu, H. Lin, and J. Wang, "Commutation error compensation strategy for sensorless brushless DC motors," *Energies*, vol. 12, no. 2, Jan. 2019, doi: 10.3390/en12020203.
- [23] J. C. Gamazo-Real, E. Vázquez-Sánchez, and J. Gómez-Gil, "Position and speed control of brushless DC motors using sensorless techniques and application trends," *Sensors*, vol. 10, no. 7, pp. 6901–6947, Jul. 2010, doi: 10.3390/s100706901.
- [24] F. Golesorkhie, F. Yang, L. Vlacic, and G. Tansley, "Field oriented control-based reduction of the vibration and power consumption of a blood pump," *Energies*, vol. 13, no. 15, Jul. 2020, doi: 10.3390/en13153907.
- [25] S.-M. Liu, C.-H. Tu, C.-L. Lin, and V.-T. Liu, "Field-oriented driving/braking control for electric vehicles," *Electronics*, vol. 9, no. 9, Sep. 2020, doi: 10.3390/electronics9091484.
- [26] C. Wu, C. Guo, Z. Xie, F. Ni, and H. Liu, "A signal-based fault detection and tolerance control method of current sensor for PMSM drive," *IEEE Transactions on Industrial Electronics*, vol. 65, no. 12, pp. 9646–9657, Dec. 2018, doi: 10.1109/TIE.2018.2813991.
- [27] H. Chuan, S. M. Fazeli, Z. Wu, and R. Burke, "Mitigating the torque ripple in electric traction using proportional integral resonant controller," *IEEE Transactions on Vehicular Technology*, vol. 69, no. 10, pp. 10820–10831, Oct. 2020, doi: 10.1109/TVT.2020.3013414.
- [28] Q. Lin, Q. Zheng, S. Miao, Y. Li, and R. Zhao, "Comparison of PMSM and BLDC applications in servo system," in *Proceedings of the International Conference of Fluid Power and Mechatronic Control Engineering (ICFPMCE 2022)*, Dordrecht: Atlantis Press International BV, 2023, pp. 67–74.
- [29] Z. Han, J. Liu, W. Yang, D. B. Pinhal, N. Reiland, and D. Gerling, "Improved online maximum-torque-per-ampere algorithm for speed controlled interior permanent magnet synchronous machine," *IEEE Transactions on Industrial Electronics*, vol. 67, no. 5, pp. 3398–3408, May 2020, doi: 10.1109/TIE.2019.2918471.
- [30] J. Jang, K. Cho, and G.-H. Yang, "Design and experimental study of dragonfly-inspired flexible blade to improve safety of drones," *IEEE Robotics and Automation Letters*, vol. 4, no. 4, pp. 4200–4207, Oct. 2019, doi: 10.1109/LRA.2019.2928773.
- [31] J. Shahid, A. Kashif, and M. K. Shahid, "A comprehensive review of physical therapy interventions for stroke rehabilitation: impairment-based approaches and functional goals," *Brain Sciences*, vol. 13, no. 5, Apr. 2023, doi: 10.3390/brainsci13050717.
- [32] M. E. Henea *et al.*, "Recovery of spinal walking in paraplegic dogs using physiotherapy and supportive devices to maintain the standing position," *Animals*, vol. 13, no. 8, Apr. 2023, doi: 10.3390/ani13081398.
- [33] D. Gomez-Vargas, M. J. Pinto-Betnal, F. Ballen-Moreno, M. Munera, and C. A. Cifuentes, "Therapy with T-FLEX ankle-exoskeleton for motor recovery: a case study with a stroke survivor," in *2020 8th IEEE RAS/EMBS International Conference for Biomedical Robotics and Biomechanics (BioRob)*, Nov. 2020, pp. 491–496, doi: 10.1109/BioRob49111.2020.9224277.
- [34] D. A. Winter, *Biomechanics and motor control of human movement*. Wiley, 2009.
- [35] A. N. Kasruddin Nasir, M. A. Ahmad, and M. O. Tokhi, "Hybrid spiral-bacterial foraging algorithm for a fuzzy control design of a flexible manipulator," *Journal of Low Frequency Noise Vibration and Active Control*, vol. 41, no. 1, pp. 340–358, Aug. 2022, doi: 10.1177/14613484211035646.
- [36] C. Lee and D. An, "AI-based posture control algorithm for a 7-DOF robot manipulator," *Machines*, vol. 10, no. 8, Aug. 2022, doi: 10.3390/machines10080651.

## BIOGRAPHIES OF AUTHORS






**Andi Nur Halisyah**    was born in Makassar, Indonesia, in 2001. She was a student at the Electrical Engineering Department, Institut Teknologi Telkom Surabaya, Indonesia. Currently looking for an opportunity for a post-graduate scholarship in the electrical engineering field with a concentration in control and automation engineering. She can be contacted by email: andinralsyih17@gmail.com.



**Dimas Adiputra**    was born in Jakarta, Indonesia, in 1993. He received a Ph.D. degree in medical instrumentation from Universiti Teknologi Malaysia, Malaysia, in 2020. He is currently an Assistant Professor at the Electrical Engineering Department, Institut Teknologi Telkom Surabaya, Indonesia. His research interests in control engineering applications include healthcare devices and the internet of things, where the ultimate goal is healthcare services or facilities that transcend the distance for everyone. He can be contacted at email: [adimas@ittelkom-sby.ac.id](mailto:adimas@ittelkom-sby.ac.id).



**Ardiansyah Al Farouq**    has proudly served as a lecturer at IT Telekom Surabaya since 2018. With a relentless passion for exploring the realms of robotics and intelligent systems, my journey in the world of academia and research has been nothing short of exhilarating. He is deeply committed to a singular, overarching mission: to enhance the quality of life by promoting relaxation and safety through cutting-edge technological innovations. He can be contacted at email: [alfarouq@ittelkom-sby.ac.id](mailto:alfarouq@ittelkom-sby.ac.id).